DOI: 10.1002/ejic.200901012

Determination of the Nature of Exchange Interactions in the 3d–4f Magnetic Chain $\{[Cu(salen)Pr(hfac)_3]_2(L)\}_n$ (L = 4,4′-Bipyridine, Pyrazine)

Fabrice Pointillart*[a,b] and Kevin Bernot[a,c]

Keywords: Copper / Nickel / Praseodymium / Crystal field / Magnetic properties

The reaction of copper(II)–praseodymium(III) 3d–4f precursors with nitrogenated ligands yields to a 3d–4f–4f–3d pseudo-1D compound with the formula $\{[\{Cu(salen)\}\{Pr(hfac)_3\}_2(pyz)](H_2O)_3\}$ (pyz = pyrazole). A "comparative method" was used to determine the nature of the magnetic interactions in this magnetic chain, by analysing the magnetic behaviour of diamagnetic or building-block analogues. This method allows the estimation of the nature of all the magnetic interactions in the compound even in the presence of the orbitally degenerate Pr^{III} ion. Two intramolecular exchange interactions [3d(Cu^{II})–4f(Pr^{III}) and 4f(Pr^{III})–4f(Pr^{III})] and one intermolecular exchange interaction [3d(Cu^{II})–3d(Cu^{II})] have been identified, and they have been found to be antiferromagnetic. The buildings blocks were obtained by reaction of Cu(salen) complexes with $Pr(hfac)_3{\cdot}3H_2O$, and the dinuclear $[Cu(salen)Pr(hfac)_3(H_2O)_n]$ {$hfac^-$ = 1,1,1,5,5,5-hexafluoroacetylacetonate, H_2salen = *N*,*N*′-ethane-1,2-diylbis(salicylidenamine), n = 0 or 1} or the heterotetranuclear $\{[\{Cu(salen)\}\{Pr(hfac)_3\}_2(bpy)](CHCl_3)_2\}$ compounds were formed. The diamagnetic analogues were obtained by substituting copper(II) by nickel(II). Evidence of a change of the crystal field around the Pr^{III} ion as a result of the presence of a nitrogenated ligand in its coordination sphere is provided. The change in the crystal field leads to a different energy distribution of the Stark sublevels and allows the determination of the Cu^{II}–Pr^{III} interaction.

Introduction

Clusters that present single molecule magnet (SMM) behaviour[1] have been a source of great interest in the field of magnetism. One of the strategies to obtain an SMM is the 3d–4f hetero-orbital approach.[2] In such a strategy, 3d metal ions are used to provide significant magnetic exchange interactions in the systems, while 4f metal ions bring great anisotropy. The association of 4f and 3d metal ions can also give a great diversity of molecular edifices, for example, the extended network based on oxamato ligand,[3] which can give rise to systems with a long-range magnetic ordering,[4] or discrete molecular systems based on Schiff bases.[5] These two examples can also be combined as in $[M(salenR)LnX_3]$ complexes {where M = Cu^{II} and Ni^{II}, salenR is the Schiff base derived from salicylaldehyde or 2-hydroxy-3-methoxybenzaldehyde, X = NO_3^-, 1,1,1,5,5,5-hexafluoroacetylacetonate ($hfac^-$) or tetramethylheptanedionate (thd^-)}.[6] Moreover, the use of bulky ligands such as $hfac^-$ or thd^- enhance the molecular magnetic properties of the clusters, as they provide good magnetic isolation of the molecules with respect to the crystal packing.[7] With this type of ligand, Gd^{III}, Dy^{III} and Tb^{III} are the most studied 4f elements, but in the majority of cases, they form dinuclear species instead of high-nuclearity complexes.[8] Most of the already reported 3d–4f compounds contain gadolinium(III) as the lanthanide counterpart since it permits the determination of the nature and magnitude of the 3d–4f magnetic exchange interaction. Studies of exchange-coupled M–Gd^{III} systems (M = Cu^{II}, Ni^{II}, Co^{II}, Fe^{III} and $V^{IV}O$) reveal that the interaction is ferromagnetic in most cases.[8–12] Additionally, from reported studies on dimeric Cu^{II}–Gd^{III} systems, it may be surmized that the ferromagnetic interactions increase with a decrease in the dihedral angle between the bridging moieties of the two metal ions.[10b,11,8c] However, the ferromagnetic behaviour is not intrinsic – it depends on the environment of the metal ions and on the structural parameters, and the interaction may even turn out to be antiferromagnetic.[13] Contrary to those of M–Gd^{III} systems, the magnetic behaviour of heterometallic complexes based on other lanthanides has been sparsely investigated. For $4f^n$ ($n < 7$) trivalent lanthanide ions, antiferromagnetic 3d–4f exchange interactions are predicted. For $4f^n$ ($n \geq 7$)[11] ions, ferromagnetic exchange interactions are expected, but reported studies do not fully corroborate this prediction.[13a,14]

[a] L.A.M.M, Department of Chemistry and INSTM Reasearch Unit,
Università di Firenze,
via Della Lastruccia 3, 50019 Sesto Fiorentino (FI), Italy
[b] Organométalliques et Matériaux Moléculaires,
UMR 6226 CNRS-UR1 Sciences Chimiques de Rennes, Université de Rennes 1,
35042 Rennes Cedex, France
Fax: +33-2-23236752
E-mail: fabrice.pointillart@univ-rennes1.fr
[c] Université Européenne de Bretagne, INSA, SCR, UMR 6226, 35043 Rennes, France

Supporting information for this article is available on the WWW under http://dx.doi.org/10.1002/ejic.200901012.

The 2p-Pr^{III} magnetic exchange interaction (where a 2p orbital comes from a nitronyl nitroxide radical) is reported to be antiferromagnetic.[15] However, to the best of our knowledge, when the 2p spin carrier is changed to a 3d ion such as Cu^{II}, the Cu^{II}–Pr^{III} interaction is found to be negligible. The question can be asked why significant magnetic exchange interactions are found in the first case and not in the second case. This can be explained by the peculiarity of the magnetism of 4f elements and, especially, by the influence of the crystal field.

The Pr^{III} ion (S = 1, L = 5, J = 4) is a non-Kramer ion,[16] and the $^3H_4$ ground state can give rise to a single ground Stark level.[14] The separation between the first excited state ($^{2S+1}L_J$) and the ground state is more than 1000 cm^{-1}.[17] The latter splits into Stark sublevels under the influence of a crystal field.[18] The crystal field effects are of the order of 100 cm^{-1} for lanthanides. When the temperature decreases, depopulation of these sublevels leads to a deviation from the Curie law, observed by a variation in the $\chi_M T$ product even in the absence of any exchange interaction. The $\chi_M T$ product can be written as: $\chi_M T = \chi_{Ln} T + J$, where J is the exchange interaction value between the Ln^{III} ion and the other paramagnetic centre. The nature of the magnetic exchange interaction cannot be determined from the shape of the experimental $\chi_M T$ curve.

A "comparative method" has already been used to determine the nature of the magnetic exchange interaction. It involves the comparison of the magnetic properties of two series of isostructural compounds, one composed of Ln–M pairs, the second of Ln–M′ pairs (M is a paramagnetic and M′ a diamagnetic 3d ion).[14,15,19–23] More recently, a quantitative determination of the crystal-field parameters for such lanthanide ions[24] has been achieved through the use of the Simple Overlap Model,[25] an extension of the purely electrostatic ligand-field theory, which takes into account some degree of covalence. In the assumption of isotropic coupling, a reasonable fit of the powder susceptibility data was realized in the cases of anisotropic lanthanide ions such as Dy^{III} and Ho^{III}.[24]

As mentioned before, the most important parameters to determine the nature of the magnetic exchange interaction that involves 4f ions is the crystal field around the 4f element. In fact it has been shown that the numbers of Stark sublevels is dependent on the symmetry of the Ln^{III} site.[26] In our family of compounds, all Pr^{III} ions present the same D_{3h} symmetry, and this allows for reasonable comparison of their magnetic properties.

This paper describes how magnetic exchange interactions have been determined in the compound {[Cu(salen){Pr(hfac)$_3$}$_2$(pyz)](H$_2$O)$_3$} {H$_2$salen = *N*,*N*′-ethane-1,2-diylbis(salicylidenamine), hfac$^-$ = 1,1,1,5,5,5-hexafluoroacetylacetonate} (noted Cu_2Pr_2pyz) and why this tetranuclear compound has to be considered as a magnetic chain. Smaller entities, i.e. building blocks, have first been characterized by X-ray diffraction and magnetic measurements. Hence, analysis of diamagnetic analogues {[Ni(salen)Pr(hfac)$_3$](H$_2$O)} (noted NiPr) and {[Ni(salen)Pr(hfac)$_3$(pyr)](CHCl$_3$)} (noted NiPrpyr) permits the estimation of the change in the Pr^{III} crystal field during passage from a fully oxygenated coordination sphere of the Pr^{III} ion (O9) to a partially nitrogenated one (NO8).

Comparison of the magnetic behaviour of NiPr with its "paramagnetic analogue" [Cu(salen)Pr(hfac)$_3$]$_2$ (noted CuPr) then gives an evaluation of the nature of the Cu^{II}–Pr^{III} exchange interaction, which was the trickiest to evaluate in this study. Next, the use of [Cu(salen)Pr(hfac)$_3$(pyr)] (noted CuPrpyr) and {[{Cu(salen)Pr(hfac)$_3$}$_2$(bpy)](CHCl$_3$)$_2$} (noted Cu_2Pr_2bpy, bpy = 4,4′-bipyridine), which present different crystal packing, allows for an estimation of the Cu^{II}–Cu^{II} intermolecular interaction. Finally, by changing the pyrazole for a bulkier nitrogenated ligand (bpy), the strictly tetranuclear complex {[{Cu(salen)Pr(hfac)$_3$}$_2$(bpy)](CHCl$_3$)$_2$} (noted Cu_2Pr_2bpy) is obtained, and the nature of the Pr^{III}–Pr^{III} magnetic exchange interaction can be determined.

Results and Discussion

Methodology and Synthesis

Some authors have used an ingenious strategy to evaluate the exchange interaction in 4f-based complexes.[14,15,19–23] This so-called "comparative method" consists of substituting pieces of complexes with its diamagnetic analogue. A step-by-step process allows the determination of the spin-orbit coupling affecting the Ln^{III} ion, and then gives the magnetic data for the whole complex free from the crystal-field effect.

A widely used precursor for building 3d–4f complexes is the Ln(hfac)$_3$·2H$_2$O salts. Indeed, the hfac$^-$ ligand is able to increase the Lewis acidity of the Ln^{III} ions[27–28] and to favour the coordination of neutral ligands. Many heterodinuclear complexes were synthesized with these precursors;[11,29] the two metals are bis-chelated, and six out of the eight bonds around the Ln^{III} ion involve the hfac$^-$ ligand. Unfortunately, these complexes cannot lead to complexes of higher nuclearity as no position remains free on the Ln^{III} ions. An exception is the [Cu(salen)La(hfac)$_3$(H$_2$O)] complex reported by Kahn and co-workers that shows a nine-coordinate La^{III} ion,[11] in which one of the positions is occupied by a water molecule and is thus supposed to be quite labile. This inspired us, as it should be possible, using appropriate ligands, to bridge two of these building blocks to give rise to extended complexes. Moreover, the easy substitution of the Ln^{III} ions should allow the replacement of La^{III} by another lanthanide ion to give a fully paramagnetic building block. In only a few tris(hexafluoroacetylacetonate)lanthanide starting complexes does the lanthanide centre have a coordination number of nine (or more) (La^{III}, Ce^{III}, Pr^{III} and in some cases Nd^{III}).[30] We chose to avoid Ce^{III} because it can be tricky to work with because of its very accessible diamagnetic oxidized form (Ce^{IV}). The Nd^{III} ion seems to be "borderline", as it can be both eight- or nine coordinated; thus a good candidate seems to be the Pr^{III} ion. Moreover, it is a non-Kramer ion, and even when antiferromagnetically coupled to the Cu moiety, it could give a nonzero ground state.

All the syntheses were performed in hot $CHCl_3$ (50–60 °C) in order to help the exchange of the coordinated molecule with the Cu(salen) precursor. Reaction between Cu(salen) and $Pr(hfac)_3{\cdot}2H_2O$ leads to the formation of a dinuclear compound with the formula $[\{Cu(salen)Pr(hfac)_3\}_2]_2$ (named CuPr). Addition of an excess of the pyrazine ligand (about 2 equiv.) leads to the anticipated tetranuclear complex with the formula $\{[\{Cu(salen)Pr(hfac)_3\}_2(pyz)](H_2O)_3\}$ (named Cu_2Pr_2pyz). We then investigated the possible cancellation of the Pr^{III}–Pr^{III} magnetic interaction as we substituted the pyrazine ligand with a similar but larger ligand, 4,4′-bypyridine. The complex obtained was $\{[\{Cu(salen)Pr(hfac)_3\}_2(bpy)](CHCl_3)_2\}$ (named Cu_2Pr_2bpy). However, the effect of the crystal field of the Pr^{III} ions on the magnetic properties of the complex has to be determined. Thus as mentioned before, diamagnetic substitution of the Cu^{II} ions was necessary. Reaction of Ni(salen) and $Pr(hfac)_3(H_2O)$ in chloroform forms unstable crystals of a supposed $[Ni(salen)Pr(hfac)_3(H_2O)]$ compound. Recrystallization in hot 1,2-dichloroethane gives stable single crystals of $\{[Ni(salen)Pr(hfac)_3(H_2O)][Ni(salen)]\}$ (noted NiPr). To perform a valuable estimation of the crystal field effect of the Pr^{III}, one as to consider a Pr^{III} ion surrounded by eight oxygen atoms and one nitrogen atom. Unfortunately, no satisfactory compounds were found in the literature. A good model, however, can be obtained by reacting NiPr with an excess of pyrazole ligand (noted pyr), which can be considered as the monodentate analogue of pyrazine. The reaction leads to $\{[Ni(salen)Pr(hfac)_3(pyr)](CHCl_3)\}$ (named NiPrPyr).

Examination of the crystal structure of the complexes Cu_2Pr_2pyz and Cu_2Pr_2bpy shows that they are not tetranuclear, but can be considered as pseudo-one-dimensional compounds. Actually, each terminal copper ion interacts with a copper ion of another complex to give a linear compound.

This forced us to find a method to estimate the interaction between those two copper ions. Fortunately, the reaction between CuPr and the pyrazole ligand led to a dinuclear compound in which no Cu^{II}–Cu^{II} interactions take place. It has the formula $[Cu(salen)Pr(hfac)_3(pyr)]$ and is named CuPrpyr. Comparison (and subtraction) of the magnetic interactions with those of Cu_2Pr_2bpy then gives the Cu^{II}–Cu^{II} magnetic exchange interaction.

We would like to stress that classic substitution of the paramagnetic ions with diamagnetic ions does not allow the determination of all the interactions in Cu_2Pr_2pyz. In fact, only a study of derivatives of the building blocks is able to give an estimation of the Cu–Pr interaction, since intermolecular interactions are present in this complex.

Description of the Structures

{[Ni(salen)Pr(hfac)$_3$][Ni(salen)]} (NiPr)

The compound NiPr crystallizes in the monoclinic system, space group *Cc* (No. 9) (Table 2). The unit cell contains two $\{[Ni(salen)Pr(hfac)_3][Ni(salen)]\}$ entities. An ORTEP[31] view is shown in the Figure 1a. The asymmetric unit is composed of two Ni(salen) moieties, one bound to the Pr^{III} ion and the other is free. On one hand, the coordination sphere of the Pr^{III} ion is completed by three bidentate $hfac^-$ ligands and one water molecule. The Pr^{III} ion is thus nine–coordinate, by oxygen atoms. The geometry around the praseodymium can be described both as a slightly distorted 4-capped square antiprism and as a 4,4,4-tricapped trigonal prism in which the distorted square face is defined by the O1–O3–O7–O8 plane and the other faces are triangular. The coordination polyhedron has a D_{3h} symmetry.[32] The Pr–O distances range from 2.415(9) to 2.567(2) Å (Table 1). All the bonds are not of similar length; in fact there are six long bonds of about 2.545(6) Å and three short bonds of about 2.434(8) Å. The shortest distance corresponds to the triangular O4–O6–O7 face of the polyhedron. On the other hand, the two nickel ions are in the N_2O_2 inner coordination site, connected in a square-planar environment to two amine nitrogen and two phenoxido oxygen atoms from the $salen^{2-}$ ligand. No differences in the Ni–X (X = O and N) bond lengths are observed when the $Pr(hfac)_3(H_2O)$ moiety is coordinated or not coordinated. The Ni–X bond lengths are similar with an average distance of 1.856(9) Å (Table 1). The Ni1–Pr1

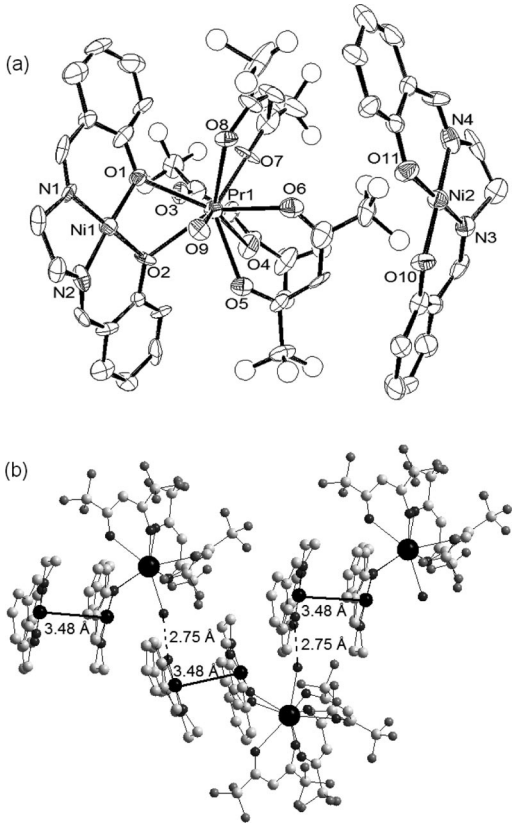

Figure 1. (a) ORTEP[31] view of the asymmetric unit of NiPr with thermal ellipsoids at 50% probability. Hydrogen atoms and thermal ellipsoids for the fluorine atoms are omitted for clarity. (b) View of the crystal packing of NiPr, which shows the short Ni(salen)–Ni(salen) (3.48 Å) contacts and the hydrogen bonds (2.75 Å).

Table 1. Selected bond lengths [Å] for compounds NiPr, NiPrpyr, CuPrpyr, Cu_2Pr_2bpy and Cu_2Pr_2pyz.

NiPr	NiPrpyr	CuPrpyr	Cu_2Pr_2bpy	Cu_2Pr_2pyz
Ni1–N1 1.829(9)	Ni1–N1 1.835(5)	Cu1–N1 1.915(9)	Cu1–N1 1.917(5)	Cu1–N1 1.941(11)
Ni1–N2 1.844(11)	Ni1–N2 1.840(4)	Cu1–N2 1.949(10)	Cu1–N2 1.928(5)	Cu1–N2 1.912(11)
Ni1–O1 1.872(7)	Ni1–O1 1.849(3)	Cu1–O1 1.916(7)	Cu1–O1 1.922(4)	Cu1–O1 1.898(7)
Ni1–O2 1.862(3)	Ni1–O2 1.848(4)	Cu1–O2 1.906(7)	Cu1–O2 1.921(3)	Cu1–O2 1.905(8)
Pr1–O1 2.518(7)	Pr1–O1 2.546(3)	Pr1–O1 2.521(6)	Pr1–O1 2.551(4)	Pr1–O1 2.534(7)
Pr1–O2 2.549(3)	Pr1–O2 2.624(4)	Pr1–O2 2.531(7)	Pr1–O2 2.539(3)	Pr1–O2 2.606(7)
Pr1–O3 2.567(2)	Pr1–O3 2.464(4)	Pr1–O3 2.541(7)	Pr1–O3 2.480(4)	Pr1–O3 2.482(7)
Pr1–O4 2.447(8)	Pr1–O4 2.537(4)	Pr1–O4 2.444(7)	Pr1–O4 2.479(4)	Pr1–O4 2.481(8)
Pr1–O5 2.536(8)	Pr1–O5 2.491(4)	Pr1–O5 2.479(7)	Pr1–O5 2.504(4)	Pr1–O5 2.472(8)
Pr1–O6 2.441(8)	Pr1–O6 2.437(4)	Pr1–O6 2.471(8)	Pr1–O6 2.457(4)	Pr1–O6 2.448(8)
Pr1–O7 2.415(9)	Pr1–O7 2.493(4)	Pr1–O7 2.468(8)	Pr1–O7 2.505(3)	Pr1–O7 2.490(6)
Pr1–O8 2.548(8)	Pr1–O8 2.452(4)	Pr1–O8 2.470(8)	Pr1–O8 2.487(3)	Pr1–O8 2.456(7)
Pr1–O9 2.551(6)	Pr1–N3 2.655(5)	Pr1–N3 2.675(10)	Pr1–N3 2.701(4)	Pr1–N3 2.747(8)
Ni2–N3 1.853(10)	Pr1–Ni1 3.270(1)	Cu1–N3 2.905(15)	Cu1–O8 2.798(9)	Cu1–O3 2.994(9)
Ni2–N4 1.860(10)		Pr1–Cu1 3.372(4)	Cu1–O1a 4.575(12)	Cu1–O1a 4.327(11)
Ni2–O10 1.851(10)		Cu1–Cu1 6.027(4)	Cu1–O2a 4.079(12)	Cu1–O2a 3.928(6)
Ni2–O11 1.873(8)			Pr1–Cu1 3.349(4)	Pr1–Cu1 3.316(2)
Pr1–Ni1 3.386(2)			Cu1–Cu1 3.730(10)	Cu1–Cu1 3.411(5)
			Pr1–Pr1a 12.487(36)	Pr1–Pr1a 8.321(14)

intramolecular distance is 3.386 Å, while the intermolecular distance between the Pr^{III} ion (Pr1) and the free Ni(salen) moieties (Ni2) is 6.105 Å.

The Ni1–Ni2 intermolecular distance is 3.475 Å. The coordinated and free Ni(salen) moieties interact through π–π stacking between the $salen^{2-}$ ligands. The Ni(salen) network forms a pseudo-1D network with the $Pr(hfac)_3$ entities on both sides (Figure 1). The free Ni(salen) and $Pr(hfac)_3(H_2O)$ moieties interact by two hydrogen bonds between the coordinated water molecule and the two phenoxido oxygen atoms. The average distance between the O9 oxygen atom of the water molecule and the two O1 and O2 phenoxido oxygen atoms of the $salen^{2-}$ ligand is 2.75 Å (Figure 1b). Finally, the shortest Pr–Pr intermolecular distance is found to be 10.571 Å, and the Pr^{III} ion in a PrO_9 environment is therefore magnetically well isolated.

{[Ni(salen)Pr(hfac)$_3$(pyr)](CHCl$_3$)} (NiPrpyr)

The compound NiPrpyr crystallizes in the triclinic system, space group $P\bar{1}$ (No. 2) (Table 2). The unit cell contains two $\{[Ni(salen)Pr(hfac)_3(pyr)](CHCl_3)\}$ entities. An ORTEP view is depicted in the Figure 2a. The two entities are related by an inversion centre localized in the middle of the Cu–Cu segment. The asymmetric unit is composed of one Ni(salen) moiety bound through two phenoxido oxygen atoms to a Pr^{III} ion and one chloroform molecule of crystallization. The coordination sphere of the Pr^{III} ion is completed by three bidentate $hfac^-$ ligands and one pyrazole molecule. The Pr^{III} ion is nine–coordinate, and the crystal field is defined by a $PrNO_8$ environment. As in NiPr, the praseodymium environment can be described as a distorted 4-capped square antiprism or better by a 4,4,4-tricapped trigonal prism with fourteen triangular faces.[32] The coordination polyhedron has a D_{3h} symmetry. The range for the Pr–O distances is 2.437(4)–2.624(4) Å (Table 2). The $Pr–O_{salen}$ [2.585(4) Å] bonds are longer than the $Pr–O_{hfac}$ bonds [2.479(4) Å]. The ninth coordination position is occupied by a nitrogen atom from the pyrazole ligand. The Pr–N3 distance is longer than all the Pr–O distances. This pyrazole ligand interacts by intramolecular hydrogen bonds (2.323 and 2.580 Å) with the perfluorated groups of $hfac^-$ ligands. The nickel ion is in the N_2O_2 inner coordination site, connected in a square-planar environment to two amine nitrogen and two phenoxido oxygen atoms from the $salen^{2-}$ ligand. The Ni–O [1.849(4) Å] and

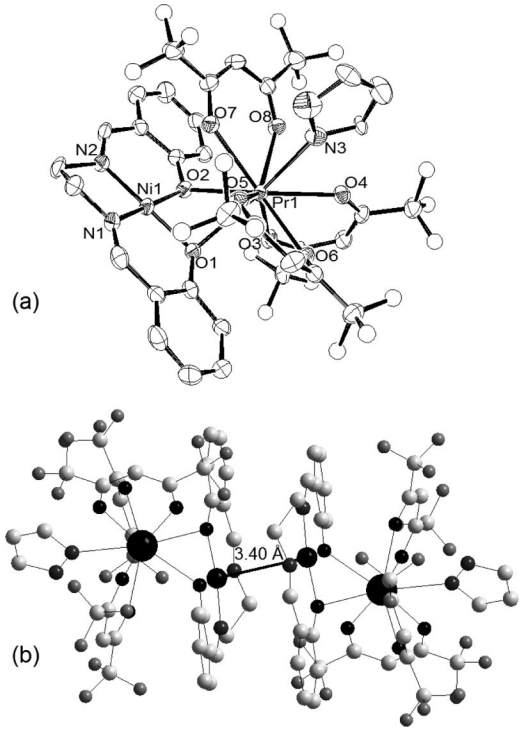

Figure 2. (a) ORTEP[31] view of the asymmetric unit of NiPrpyr with thermal ellipsoids at 50% probability. Hydrogen atoms, the chloroform molecule of crystallization and thermal ellipsoids for the fluorine atoms are omitted for clarity. (b) View of the crystal packing for two asymmetric units of NiPrpyr, which shows the short Ni(salen)–Ni(salen) (3.40 Å) contact.

Ni–N [1.838(5) Å] bond lengths are similar. The intramolecular Ni–Pr distance is 3.270 Å. The intermolecular Ni–Ni and Pr–Pr distances are 3.395 and 9.132 Å, respectively (Figure 2b). The chloroform molecule is quite far, >4 Å, from the nearest atom of the dinuclear species Ni(salen)-$Pr(hfac)_3(pyr)$,; this solvent molecule can therefore easily evaporate, and this is probably the reason why the single crystals are unstable. The crystallographic structure of NiPrpyr attests that the reaction in $CHCl_3$ of Ni(salen)Pr-$(hfac)_3(H_2O)$ with excess pyrazole leads to the substitution of the water molecule by a pyrazole molecule. However, the coordination position of the pyrazole ligand differs from that of the water molecule in NiPr. The Pr^{III} ion in a $PrNO_8$ environment is magnetically well isolated.

[Cu(salen)Pr(hfac)$_3$]$_2$ (CuPr)

The compound CuPr crystallizes in the monoclinic system, space group $P2_1/n$ (No. 14) (Table 2). An ORTEP[31] view of the corresponding asymmetric unit is shown in Figure S1a, the short Cu–Cu intermolecular interaction is highlighted in the Figure S1b and selected distances are reported in the Table S1 (see Supporting Information). An ORTEP[31] view is shown in the Figure 3a. The asymmetric unit is composed of one Cu(salen) moiety bound to one Pr^{III} ion. The Cu^{II} and Pr^{III} ions are linked by two phenoxido oxygen atoms, the dihedral angle is 156.6° and the Cu–Pr intramolecular distance is 3.372 Å. The coordination sphere of the Pr^{III} ion is the same that in NiPrpyr with one $salen^{2-}$, three $hfac^-$ and one pyrazole ligands. The polyhedron around the Pr^{III} ion is almost the same as that in the dinuclear complex NiPrpyr. The $Pr–O_{hfac}$ [2.479(7) Å] bonds are smaller than the $Pr–O_{salen}$ [2.527(8) Å] bonds, and the Pr–N3 [2.675(10) Å] bond is longer than all the Pr–O distances. All the Pr–X distances in CuPrpyr are very similar to the Pr–X distances found in the dinuclear compound NiPrpyr. The copper ion is in the N_2O_2 inner coordination site, connected in a pseudo-square-pyramidal environment to two amine nitrogen and two phenoxido oxygen atoms from the $salen^{2-}$ ligand and one nitrogen atom from the pyrazole ligand [Cu–N3 2.905(15) Å] (Figure 3b). The $Cu–X_{square\text{-}plane}$ [1.922(8) Å] bond lengths are equal and are longer than the Ni–X distances [1.844(4) Å] in NiPrpyr. This increase in the bond lengths may be due to the difference in the electronic configuration between a Cu^{II} ion [$3d^9$, $(t_{2g})^6(e_g^*)^3$] and a Ni^{II} ion [$3d^8$, $(t_{2g})^6(e_g^*)^2$].

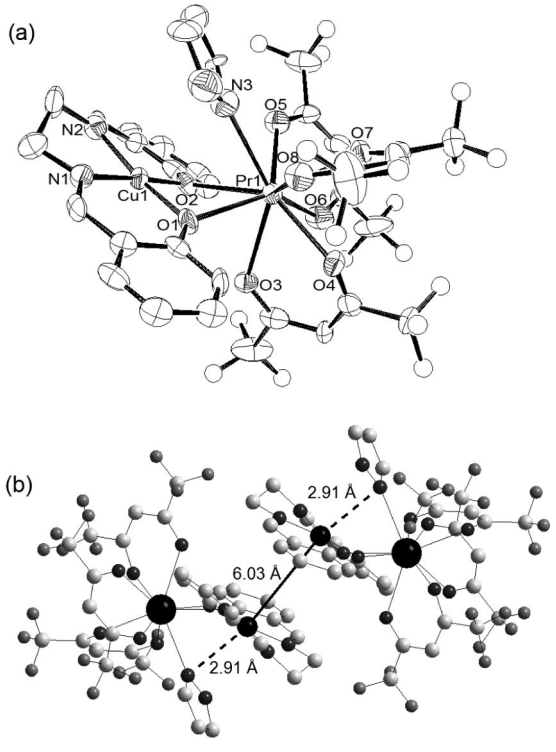

Figure 3. (a) ORTEP[31] view of the asymmetric unit of CuPrpyr with thermal ellipsoids at 50% probability. Hydrogen atoms and thermal ellipsoids for the fluorine atoms are omitted for clarity. (b) View of the crystal packing for two asymmetric units of CuPrpyr, which shows the long Cu(salen)–Cu(salen) (6.03 Å) distance and the short contacts between the Cu^{II} ions and the pyrazole ligands.

[Cu(salen)Pr(hfac)$_3$(pyr)] (CuPrpyr)

The compound CuPrpyr crystallizes in the monoclinic system, space group $C2/c$ (No. 15) (Table 2). The unit cell contains four [Cu(salen)Pr$(hfac)_3$(pyr)] entities. The antibonding orbital of the Cu^{II} ion has three electrons, whilst that of the Ni^{II} ion has only two; therefore, the Cu–X bonds are longer than the Ni–X bonds. Another difference between the CuPrpyr and NiPrpyr dinuclear compounds is the coordination position of the pyrazole ligand. In NiPrpyr, one $hfac^-$ anion is stacked between the pyrazole and the Ni(salen) moiety, whereas in CuPrPyr, the pyrazole is directly next to Cu(salen) to produce a short N3···Cu^{II} contact. The Cu^{II} is indeed in the centre of a pseudo-square-pyramid, which it favours. The atoms of two Schiff bases belonging to the same molecule are located in two parallel planes. The salen planes belonging to two different molecules are parallel as a result of the van der Waals interactions. The resulting Cu–Cu intermolecular distance is 6.027 Å, and the shortest Pr–Pr intermolecular distance is 9.807 Å. The dinuclear compound CuPrpyr can therefore be considered well isolated, which occurs as a result of the coordination of the pyrazole ligand. This is confirmed by the crystallographic structure of CuPr. This compound is an intermediate in the reaction leading to CuPrpyr. Its structure reveals a short Cu–Cu intermolecular interaction of 3.528 Å (Figure S2).

{[Cu(salen){Pr(hfac)$_3$}$_2$(bpy)](CHCl$_3$)$_2$} (Cu$_2$Pr$_2$bpy)

The compound Cu_2Pr_2bpy crystallizes in the triclinic system, space group $P\bar{1}$ (No. 2) (Table 2). The unit cell contains four {[Cu(salen)Pr$(hfac)_3$$(bpy)_{0.5}$](CHCl$_3$)} entities. An ORTEP[31] view is shown in the Figure 4a. The asymmetric unit is composed of one Cu(salen) moiety bound to one Pr^{III} ion. The Cu^{II} and Pr^{III} are linked by two phenoxido oxygen atoms, the dihedral angle is 149.1° and the Cu–Pr intramolecular distance is 3.349 Å (Table 1). The Pr^{III} ion is surrounded by the Cu(salen) moiety, three $hfac^-$ ligands and one 4,4′-bipyridine ligand. The tetranuclear complex is generated by an inverse centre located in the

middle of the C–C bond that links the two aromatic rings of the 4,4′-bipyridine. The six Pr–O_{hfac} bond lengths are equal [2.485(4) Å] and shorter than the two Pr–O_{salen} [2.546(4) Å] bonds, while the Pr–N3 [2.702(4) Å] distance is longer than all the Pr–O distances. The O_8N polyhedron around the Pr^{III} ion can be described by a quasi-regular, 4-capped square-antiprism geometry as a result of a nearly full detriangulation of the tricapped trigonal prism. The praseodymium ion is in a D_{3h} symmetry. The copper ion is in the N_2O_2 inner coordination site, connected in a pseudo-square-pyramidal environment to two amine nitrogen and two phenoxido oxygen atoms from the $salen^{2-}$ ligand and one oxygen atom from an $hfac^-$ ligand [Cu–O8 2.798(9) Å] (Figure 4b). Contrary to the observation in the eight-coordinate lanthanide ions, no coordination of the 4,4′-bipyridine ligand is observed in the axial position of the Cu^{II} ion because of the pseudo-square-pyramidal geometry in the presence of the coordinated $Pr(hfac)_3L$ moiety. This geometry results from the occupation of the axial position of Cu^{II} by one of the carbonyl functional groups of one $hfac^-$ ligand. This is quite different from that observed in the dinuclear complex based on $Gd(hfac)_3$, published by O. Kahn and co-workers, in which a 1-methylimidazole ligand is coordinated in the axial position of the Cu^{II} ion.[11] Actually, when the $Ln(hfac)_3$ moiety is replaced by a $Ln(NO_3)_3$ unit, the coordination of a neutral Lewis base is possible in the axial position of the Cu(salen) moiety.[33] This result is possible for two reasons: (a) the nitrate anion is smaller than the $hfac^-$ anion, and (b) the substitution of a nitrate anion by a neutral Lewis base seems to be quite difficult and this may be the reason why no example of such a reaction is reported in the literature for lanthanide ions. In our case, the 4,4′-bipyridine ligand bridges the two Pr^{III} ions, which leads to a Pr1–Pr1a intramolecular distance (12.487 Å) that is longer than the Pr1–Pr1a intermolecular distance (9.255 Å). The bridging ligand is coordinated in the position opposite to that of the Cu(salen) moiety in the NiPrpyr dinuclear complex. This conformation leads to a short Cu–Cu intermolecular distance of 3.73 Å. On the contrary, when the additional ligand is coordinated in close proximity to the Cu(salen) moiety (like in CuPrpyr), the Cu–Cu intermolecular distance is long. Both extremities of the tetranuclear complex are in short contact with other tetranuclear units, and the compound Cu_2Pr_2bpy can be described as a quasi-one-dimensional compound.

{[{Cu(salen)Pr(hfac)$_3$}$_2$(pyz)](H$_2$O)$_3$} (Cu$_2$Pr$_2$pyz)

The compound Cu_2Pr_2pyz crystallizes in the monoclinic system, space group *C*2/*c* (No. 15) (Table 2). The unit cell contains four $\{[Cu(salen)Pr(hfac)_3(pyz)_{0.5}](H_2O)_{1.5}\}$ entities. An ORTEP[31] view is shown in the Figure 5a. The crystallographic structure is similar to that of Cu_2Pr_2bpy, the asymmetric unit is composed of one Cu(salen) moiety bound to one $Pr(hfac)_3(pyz)$ moiety. The two dimers are linked by two phenoxido oxygen atoms, the dihedral angle is 145.6° and the Cu–Pr intramolecular distance is 3.316 Å. The Cu–X and Pr–X distances are almost similar to the those in heterotetranuclear Cu_2Pr_2bpy (Table 1). The pyrazine ligand is coordinated in the same position as the bipyridine in Cu_2Pr_2bpy. However, this short bridging ligand leads to a Pr1–Pr1 intramolecular distance of 8.321 Å (compare to 12.487 Å for the Cu_2Pr_2bpy compound), which

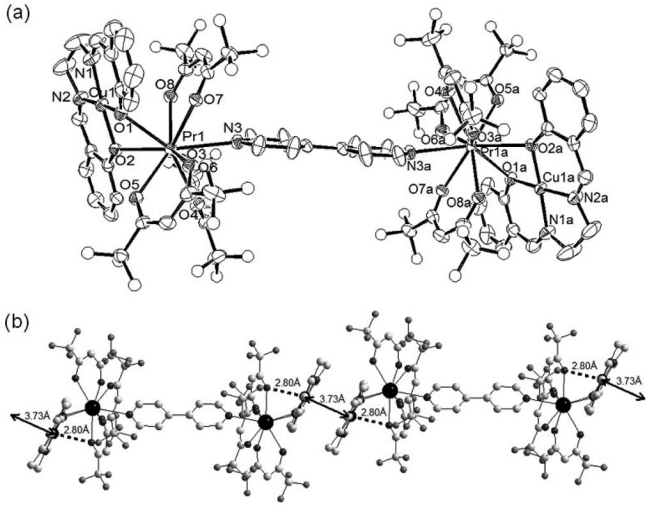

Figure 4. (a) ORTEP[31] view of the tetranuclear compound Cu_2Pr_2bpy with thermal ellipsoids at 50% probability. Hydrogen atoms, chloroform molecules and thermal ellipsoids for the fluorine atoms are omitted for clarity. (b) View of the crystal packing of Cu_2Pr_2bpy, which shows the short Cu(salen)–Cu(salen) (3.73 Å) and Cu(salen)–O_{hfac} (2.80 Å) contacts highlighting the quasi-one-dimensional structure.

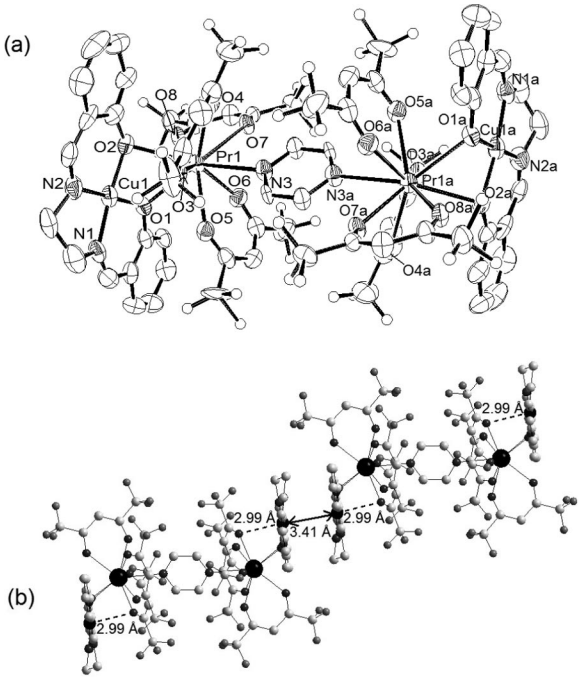

Figure 5. (a) ORTEP[31] view of the tetranuclear compound Cu_2Pr_2pyz with thermal ellipsoids at 50% probability. Hydrogen atoms, water molecules and thermal ellipsoids for the fluorine atoms are omitted for clarity. (b) View of the crystal packing of Cu_2Pr_2pyz, which shows the short Cu(salen)–Cu(salen) (3.41 Å) and Cu(salen)–O_{hfac} (2.99 Å) contacts highlighting the quasi-one-dimensional structure.

is, in this case, shorter than the Pr–Pr intermolecular distance (9.248 Å). As for Cu_2Pr_2bpy, the coordination position of the pyrazine ligand induces a short Cu–Cu intermolecular distance (3.411 Å) (Figure 5b). Thus, Cu_2Pr_2pyz can be also described as a quasi-one-dimensional compound.

In summary, the structure of a dinuclear complex (NiPr) incorporating a Pr^{III} ion in a PrO_9 environment and a diamagnetic ion (Ni^{II}) is described and discussed. Furthermore, the substitution of one water molecule by a pyrazole ligand gives rise to two dinuclear complexes NiPrpyr and CuPrpyr having a Pr^{III} ion in a PrO_8N environment. In the first complex, the Pr^{III} ion is associated to a diamagnetic Ni^{II} ion, while in the second complex, it is associated to a paramagnetic Cu^{II} ion. In contrast to the intermediate compound CuPr, CuPrpyr is well isolated. Finally, the crystal structures of two heterotetranuclear complexes (Cu_2Pr_2bpy and Cu_2Pr_2pyz) are described and discussed. The crystal structure of these compounds can be considered to be one dimensional in which the Pr^{III} ion is in a PrO_8N environment and is associated to a paramagnetic Cu^{II} ion. In all the reported compounds, the distances, angles, symmetries (D_{3h}) and geometries (4,4,4-tricapped trigonal prism) involving the metallic ions (Ni^{II}, Cu^{II} and Pr^{III}) are similar. The magnetic data were analyzed by using the "comparative method".

Magnetic Properties

The crystallographic analysis of the Cu_2Pr_2pyz complex reveals that the structure can be described as a quasi-one-dimensional compound. However, from a magnetic point of view, the structure is a one-dimensional system (Figure 6a).

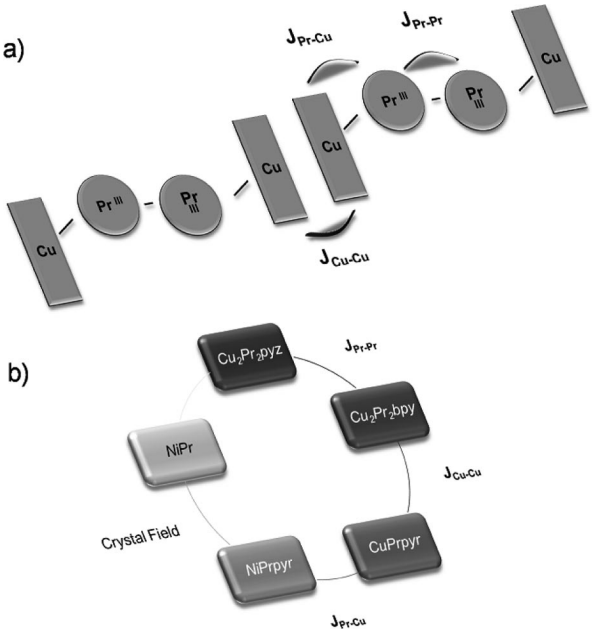

Figure 6. (a) Scheme for the one-dimensional magnetic structure of Cu_2Pr_2pyz, which shows the 3d–4f ($J_{Cu\text{-}Pr}$), 3d–3d ($J_{Cu\text{-}Cu}$) and 4f–4f ($J_{Pr\text{-}Pr}$) exchange interactions. (b) Scheme of the useful complexes for and the parameters determined by the comparative method.

Three different magnetic exchange interactions may occur in this chain: (1) one 3d–4f exchange interaction between the Cu^{II} and Pr^{III} ions through the bridging phenoxido oxygen atoms, $J_{Cu\text{-}Pr}$, (2) one intermolecular 3d–3d exchange interaction between two stacked Cu(salen) moieties, $J_{Cu\text{-}Cu}$, and (3) one 4f–4f exchange interaction between two Pr^{III} ions through the bridging pyrazine ligand, $J_{Pr\text{-}Pr}$. Schemes for the magnetic structure of Cu_2Pr_2pyz and of the comparative method is shown on the Figure 6.

Magnetic Properties of NiPr and NiPrpyr: Observation of the Crystal-Field Effect in an O9 and O8N Environment

Figure 7 shows the $\chi_M T$ vs. T plot for the two compounds NiPr and NiPrpyr. For NiPr, the value at room temperature is 1.50 $cm^3 K mol^{-1}$, which is slightly lower than that expected for a free Pr^{III} ion (1.60 $cm^3 K mol^{-1}$). The $(\chi_M T)_{NiPr}$ vs. T curve shows a monotonic decrease when the sample is cooled down to 2.5 K. At this temperature, the product $(\chi_M T)_{NiPr}$ is 0.26 $cm^3 K mol^{-1}$. The shape of the $(\chi_M T)_{NiPrpyr}$ vs. T curve for NiPrpyr is similar to that of NiPr, but the values at room- and at low temperatures are slightly different, 0.35 and 1.63 $cm^3 K mol^{-1}$, respectively.

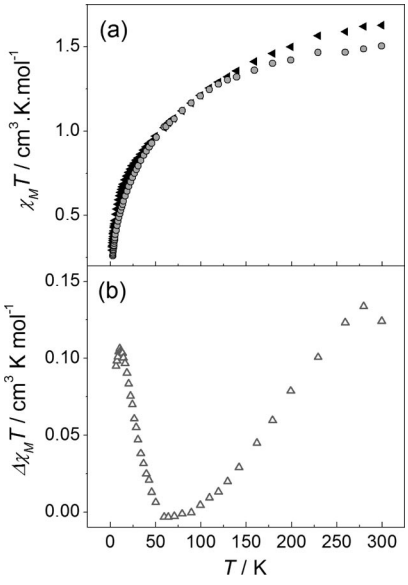

Figure 7. (a) Thermal variation of $\chi_M T$ in the temperature range 2.5–300 K in a 2000 G external field for NiPr (circles) and NiPrpyr (filled triangles). (b) Thermal variation of $\Delta\chi_M T = (\Delta\chi_M T)_{NiPrpyr} - (\Delta\chi_M T)_{NiPr}$.

In both NiPr and NiPrpyr dinuclear complexes, the Pr^{III} ion is magnetically isolated, and the monotonic decrease can be attributed to the crystal-field effect. To explain the slight variation in the $\chi_M T$ value at room temperature, one has to consider the crystal field around the Pr^{III} ion in NiPr. A value of 1.60 $cm^3 K mol^{-1}$ is given for a "free Pr^{III} ion", which corresponds to a $Pr(H_2O)_9^{3+}$ complex. $Pr(hfac)_3 \cdot 3H_2O$ entities can also be treated in such a way since the surroundings of the Pr^{III} ions are similar, i.e. $d(Pr–O_{H2O}) = d(Pr–O_{hfac})$, and the experimental value of $\chi_M T_{300K}$ is also 1.6 $cm^3 K mol^{-1}$. In the case of NiPr, the crystal structure

reveals that the Pr–O_{salen} distances are longer than the Pr–O_{hfac} distances, so the crystal field affecting the Pr^{III} ion in NiPr can be expected to be lower than for $Pr(hfac)_3{\cdot}3H_2O$. For NiPrpyr, a fundamental change occurs because the Pr^{III} ion is in a PrO_8N environment, which leads to a stronger crystal field than for a PrO_9 environment. Hence a variation in the energy distribution of the Stark sublevels is expected because of the substitution of one water molecule by one pyrazole ligand. This therefore affects the shape of the $\chi_M T(T)$ curve. This is evidenced in Figure 7b, where the $\Delta\chi_M T$ vs. T plot is depicted, [$\Delta\chi_M T = (\chi_M T)_{NiPrpyr} - (\chi_M T)_{NiPr}$].

The variation of the magnetic susceptibility as a function of the crystal field illustrates the fact that the 4f electrons can be polarized.[34] The polarization depends on the nature of the coordinated atoms (oxygen or nitrogen), and therefore some consequences on the spectroscopic measurements (absorption, emission, magnetic susceptibility and NMR) can be expected. From the magnetic point of view, the low-temperature region has to be considered as the 4f–3d and 4f–4f magnetic exchange interactions are expected to be of this order of magnitude.

Magnetic Properties of NiPrpyr and CuPrpyr: Determination of $J_{Pr\text{-}Cu}$

Figure 8 shows the $\chi_M T$ vs. T plot for the compounds NiPrpyr and CuPrpyr. The $(\chi_M T)_{NiPrpyr}$ experimental curve has been described previously. For CuPrpyr, the $(\chi_M T)_{CuPrpyr}$ vs. T curve shows a monotonic decrease from room temperature down to 2.5 K. The value of $(\chi_M T)_{CuPrpyr}$ at 300 K is 2.03 $cm^3\,K\,mol^{-1}$ and 0.45 $cm^3\,K\,mol^{-1}$ at 2.5 K. This is in agreement with the value obtained for NiPrpyr, i.e. a Pr^{III} ion in a PrO_8N environment ($\chi_M T$ = 1.63 $cm^3\,K\,mol^{-1}$) and one Cu^{II} ion (S = 1/2, g = 2.10). The crystal structure shows that CuPrpyr is a well-isolated dinuclear complex. Hence, we assume that the thermal variation of $(\chi_M T)_{CuPrpyr}$ is due both to the crystal-field effect of the Pr^{III} ion and intramolecular magnetic exchange interaction with the Cu^{II} ion. Here, we can neglect the variation in the crystal field of Pr^{III} between the two complexes NiPrpyr and CuPrpyr. The expression of the product $(\chi_M T)_{CuPrpyr}$ can be written as:

$$(\chi_M T) = (\chi_M T)_{NiPrpyr} + (\chi_M T)_{Cu} + J_{Cu\text{-}Pr}$$

$\Delta(\chi_M T)$ is defined by the following expression:

$$\Delta(\chi_M T) = (\chi_M T)_{CuPrpyr} - (\chi_M T)_{NiPrpyr} = (\chi_M T)_{Cu} + J_{Cu\text{-}Pr}$$

Figure 8b shows the thermal variation of $\Delta(\chi_M)$ and $\Delta(\chi_M T)$. The $\Delta(\chi_M T)$ value is constant from 300 to 125 K and then decreases. The value of $\Delta(\chi_M T)$ at 300 K is 0.41 $cm^3\,K\,mol^{-1}$, which corresponds to S = 1/2 and g = 2.10. These values are in agreement with those reported for Cu(salen) complexes.[11,35] It is known that $(\chi_M T)_{Cu}$ for such complexes takes on a quasi-constant value in the studied temperature range. The decrease in $\Delta(\chi_M T)$ is attributed to an antiferromagnetic exchange interaction between the Cu^{II} and the Pr^{III} ion through the two phenoxido oxygen atoms.

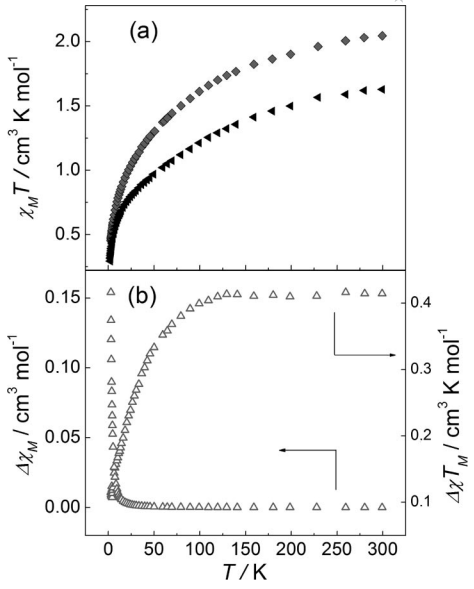

Figure 8. (a) Thermal variation of $\chi_M T$ in the temperature range 2.5–300 K in a 2000 G external field for NiPrpyr (filled black triangles) and CuPrpyr (filled grey diamonds). (b) Thermal variation of $\Delta\chi_M T = (\chi_M T)_{CuPrpyr} - (\chi_M T)_{NiPrpyr} = (\chi_M T)_{Cu} + J_{Cu\text{-}Pr}$.

The field dependence of the magnetization of NiPrpyr, CuPrpyr and the uncorrelated spin system is shown in Figure 9. The magnetization of the uncorrelated spin system was obtained by adding the field dependence of the magnetization of one Cu^{II} ion (S = 1/2, g = 2.10) at 2 K to the magnetization of NiPrpyr. The magnetization at of the Cu^{II} ion is calculated by the following Brillouin function:[17]

$$M = Ng\beta SB_s(y)$$

with $y = \dfrac{g\beta SH}{kT}$

and $B_s(y) = \dfrac{2S+1}{2S}\coth\left(\dfrac{2S+1}{2S}y\right) - \dfrac{1}{2S}\coth\left(\dfrac{1}{2S}y\right)$

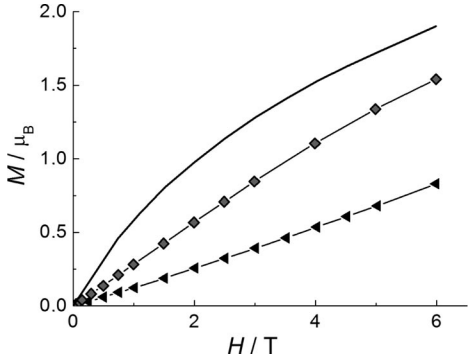

Figure 9. Experimental field dependence of the magnetization for NiPrpyr (filled black triangles), CuPrpyr (filled grey diamonds) and calculated magnetization for the uncorrelated spin system (black line). Field range 0–6 Tesla at 2 K.

For any field, the experimental magnetization of CuPrpyr is lower than that of the uncorrelated system. This comparison confirms that the Cu^{II}–Pr^{III} exchange interaction is antiferromagnetic.

Magnetic Properties of CuPrpyr and Cu_2Pr_2bpy: Determination of $J_{Cu\text{-}Cu}$

Figure 10a shows the $\chi_M T$ vs. T plot for CuPrpyr and Cu_2Pr_2bpy. The $(\chi_M T)_{CuPrpyr}$ experimental curve has been described previously in this article. The $(\chi_M T)_{Cu2Pr2bpy}$ vs. T curve is reported for two Cu^{II} and two Pr^{III} magnetic centres. The curve shows a monotonic decrease down to 2.5 K. The value of $(\chi_M T)_{Cu2Pr2bpy}$ at 300 K is 4.01 $cm^3 K mol^{-1}$ and 0.75 $cm^3 K mol^{-1}$ at 2.5 K. Previous papers show that the magnetic exchange interaction transmitted by the 4,4′-bipyridine bridging ligand is negligible.[33] Hence, the decrease in $(\chi_M T)_{Cu2Pr2bpy}$ is attributed to the crystal-field effect of the Pr^{III} ion, the intramolecular exchange interaction between the Cu^{II} and Pr^{III} ions and the intermolecular exchange interaction between the two Cu^{II} ions. The structural variation in the surroundings of both the Cu^{II} and Pr^{III} ions between the two complexes CuPrpyr and Cu_2Pr_2bpy can be neglected. The expression of the product $(\chi_M T)_{Cu2Pr2bpy}$ can be written as:

$$\Delta(\chi_M T)_{Cu2Pr2bpy} = 2[(\chi_M T)_{NiPrpyr} + (\chi_M T)_{Cu} + J_{Cu\text{-}Pr}] + J_{Cu\text{-}Cu} = 2(\chi_M T)_{CuPrpyr} + J_{Cu\text{-}Cu}$$

$\Delta(\chi_M T)$ is then defined by the following expression:

$$\Delta(\chi_M T) = (\chi_M T)_{Cu2Pr2bpy} - 2(\chi_M T)_{CuPrpyr} = J_{Cu\text{-}Cu}$$

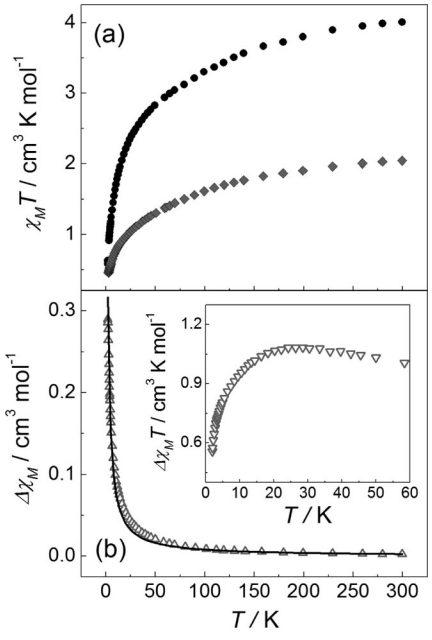

Figure 10. (a) Thermal variation of $\chi_M T$ in the temperature range 2.5–300 K in a 2000 G external field for CuPrpyr (full grey diamonds) and Cu_2Pr_2bpy (filled black circles). (b) Thermal variation of $\Delta\chi_M T = (\Delta\chi_M T)_{Cu2Pr2bpy} - 2(\Delta\chi_M T)_{CuPrpyr} = J_{Cu\text{-}Cu}$ and the best fit. A value of 0.83 $cm^3 K mol^{-1}$ has been added to the $\Delta\chi_M T(T)$ curve to represent the spin-only contribution of the two Cu^{II} centres ($S = 1/2$, $g = 2.10$).

Hence the $\Delta(\chi_M T)$ values are considered to be free of the crystal-field effect of the Pr^{III} ion and of the magnetic exchange between the Cu^{II} and Pr^{III} ions.

Figure 10b shows the thermal variation of $\Delta(\chi_M)$ and $\Delta(\chi_M T)$ with the added contribution of the two Cu^{II} ($S = 1/2$, $g = 2.10$). This method has recently been employed to determine the magnetic interactions in [(cyclam)M{(μ-Cl)-U(MePz)$_4$}$_2$] (where cyclam = 1,4,8,11-tetraazacyclotetradecane; $MePz^-$ = 3,5-dimethylpyrazolate).[36] The $\Delta(\chi_M T)$ vs. T curve shows a linear increase from 0.75 $cm^3 K mol^{-1}$ to 1.08 $cm^3 K mol^{-1}$ at 25 K and the $\Delta(\chi_M T)$ values decrease rapidly for lower temperatures. The value at room temperature is slightly lower than the expected value for two Cu^{II} ions ($S = 1/2$, $g = 2.10$), but no pertinent explanation can be found for the linear increase. Such behaviour has already been observed in a similar application of the "empirical method".[14] The decrease in the $\Delta(\chi_M T)$ vs. T curve is attributed to an antiferromagnetic intermolecular exchange interaction between the Cu^{II} ions. To estimate the intensity of this antiferromagnetic interaction, a fit of the $\Delta(\chi_M)$ was performed by using the well-known Bleaney–Bowers equation:[17]

$$\chi_M = \left[\frac{2Ng^2\beta^2}{kT\{3 + \exp(-J_{Cu\text{-}Cu}/kT)\}}\right]$$

with $H = -JS_{Cu} \cdot S_{Cu}$

The best fit ($R = 0.987$) is shown in Figure 10b, and $J_{Cu\text{-}Cu}$ is –1.86 cm^{-1} with $g_{Cu} = 2.10$. The presence of magnetic intermolecular exchange interactions between the two Cu(salen) moieties have been observed in several compounds.[9,11] Moreover, in the Cu(salen)La(hfac)$_3$(H_2O) dinuclear complex described by O. Kahn and co-workers, a very weak ferromagnetic interaction (0.2 cm^{-1}) was found. The change in the nature of the magnetic exchange interaction can be attributed to the important structural variation between the reported compound and our trinuclear compound. In fact, a slight structural change in the Cu(salen) moieties, and in the manner they stack, can lead to a modification of the nature of the magnetic interaction. Such a variation was also observed in $[Mn(salenR)]_2^{2+}$ dinuclear complexes.[37]

Magnetic Properties of Cu_2Pr_2bpy and Cu_2Pr_2pyz: Determination of $J_{Pr\text{-}Pr}$

Figure 11 shows the $\chi_M T$ vs. T plot for Cu_2Pr_2bpy and CuPrpyr. The $(\chi_M T)_{Cu2Pr2bpy}$ experimental curve has been described previously in this paper. The shape of the $(\chi_M T)_{Cu2Pr2pyz}$ curve is almost identical to that of $(\chi_M T)_{Cu2Pr2bpy}$. The values of $(\chi_M T)_{Cu2Pr2pyz}$ at 300 K and 2.5 K are 3.99 and 0.86 $cm^3 K mol^{-1}$, respectively. The magnetic exchange interaction between the two Pr^{III} ions through the bridging pyrazine ligand is expected to be weak but not negligible.[38] Therefore, the decrease in $(\chi_M T)_{Cu2Pr2pyz}$ is attributed to the crystal-field effect of the Pr^{III} ion, the intramolecular exchange interaction between the Cu^{II} and Pr^{III} ions and the intermolecular exchange interaction between the Cu^{II} ions (Figure 6).

The structural variation of the surroundings of both the Cu^{II} and Pr^{III} ions between the two complexes Cu_2Pr_2bpy and Cu_2Pr_2pyz can be neglected. The expression of the product $(\chi_M T)_{Cu2Pr2pyz}$ can be written as:

$$\Delta(\chi_M T)_{Cu2Pr2pyz} = 2[(\chi_M T)_{NiPrpyr} + (\chi_M T)_{Cu} + J_{Cu\text{-}Pr}] + J_{Cu\text{-}Cu} + J_{Pr\text{-}Pr}$$

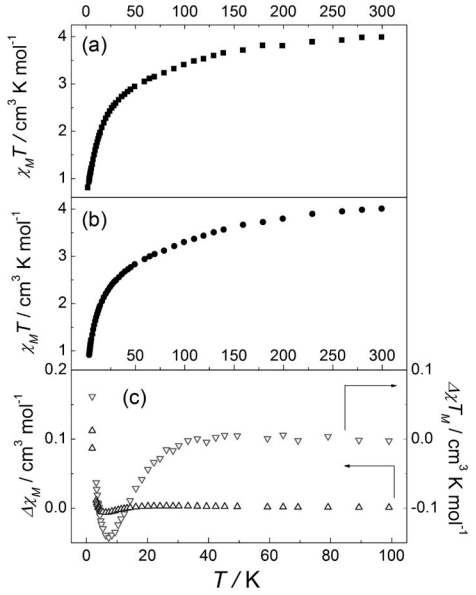

Figure 11. (a) Thermal variation of $\chi_M T$ in the temperature range 2.5–100 K in a 2000 G external field for Cu_2Pr_2pyz (filled black squares) and Cu_2Pr_2bpy (filled black circles). (b) Thermal variation of $\Delta\chi_M T = (\Delta\chi_M T)_{Cu2Pr2pyz} - (\Delta\chi_M T)_{Cu2Pr2bpy} - J_{Pr\text{-}Pr}$.

$\Delta(\chi_M T)$ is defined by the following expression:

$$\Delta(\chi_M T) = (\chi_M T)_{Cu2Pr2pyz} - (\chi_M T)_{Cu2Pr2bpy} = J_{Pr\text{-}Pr}$$

So the values of $\Delta(\chi_M T)$ are considered to be free of the crystal-field effect of the Pr^{III} ion and the magnetic exchange between (a) the Cu^{II} and Pr^{III} ions and (b) the Cu^{II} ions. Figure 11c shows the thermal variation of $\Delta(\chi_M)$ and $\Delta(\chi_M T)$. The $\Delta(\chi_M T)$ value is constant at about 0 $cm^3 K mol^{-1}$ from 300 K to 25 K, decreases from 25 to 5 K and finally increases at very low temperatures. The determination of the nature of the magnetic interaction between the two Pr^{III} ions is not so easy because $\Delta(\chi_M T)$ does not show a monotonic behaviour. The decrease between 25 and 5 K could be attributed to the magnetic exchange interaction between the Pr^{III} ions. The increase in $\Delta\chi_M$ below 5 K could be attributed to the fact that small structural variations are no longer negligible when the magnetic exchange interactions investigated become very weak.

The field dependence of the magnetization for Cu_2Pr_2pyz, Cu_2Pr_2bpy, CuPrpyr (in this case, the values of the magnetization are multiplied by two for comparison with the first magnetization of the other complexes) and for the uncorrelated spin system are shown in Figure 12. The magnetization of the uncorrelated spin system was obtained by adding the field dependence of the magnetization of two Cu^{II} ions ($S = 1/2$, $g = 2.10$) at 2 K to the two magnetization contributions of NiPrpyr. The magnetization of the Cu^{II} ions is calculated by the Brillouin function.[17] The experimental magnetization of the three complexes Cu_2Pr_2pyz, Cu_2Pr_2bpy, CuPrpyr are lower than that of the uncorrelated system.

This comparison confirms that antiferromagnetic interactions are present in the three complexes Cu_2Pr_2pyz, Cu_2Pr_2bpy and CuPrpyr. Moreover, the experimental magnetization for CuPrpyr is lower than that for Cu_2Pr_2bpy, which is lower than that for Cu_2Pr_2pyz, and agrees with the fact that the three Cu^{II}–Pr^{III}, Cu^{II}–Cu^{II} and Pr^{III}–Pr^{III} exchange interactions are antiferromagnetic.

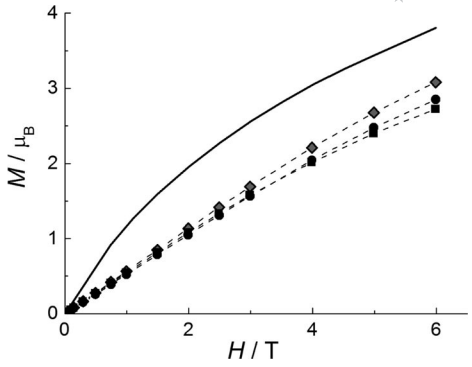

Figure 12. Experimental field dependence of the magnetization for CuPrpyr (two contributions, filled grey diamonds), Cu_2Pr_2bpy (filled black circles), Cu_2Pr_2pyz (filled black squares) and the calculated magnetization for the uncorrelated spin system (black line). Field range 0–6 Tesla at 2 K.

In this work, the nature of all the magnetic interactions in the Cu_2Pr_2pyz pseudochain has been determined by using an extension of the "empirical method". However, we think that such methodology has to be used as a qualitative investigation only because of the numerous approximations that are implied in the description of the magnetic exchange interactions and in the description of the surroundings of the magnetic ions used (considered here as strictly identical). Nevertheless, it allows for the determination that the Cu^{II}–Pr^{III}, Pr^{III}–Pr^{III} and Cu^{II}–Cu^{II} magnetic exchange interactions are antiferromagnetic and for the estimation of the latter interaction ($J_{Cu\text{-}Cu} = -1.86$ cm^{-1}).

Conclusions

The tetranuclear complex $\{[Cu(salen)\{Pr(hfac)_3\}_2(pyz)](H_2O)_3\}$ (Cu_2Pr_2pyz) has been synthesized by using the dinuclear complex $[Cu(salen)Pr(hfac)_3]$ (CuPr) and the nitrogenated pyrazine ligand. X-ray diffraction reveals that the Cu_2Pr_2pyz complex can be described as a quasi-1D compound. From a magnetic point of view, Cu_2Pr_2pyz is a strictly one-dimensional structure in which three different magnetic exchange interactions are identified: one intermolecular 3d(Cu^{II})–3d(Cu^{II}) magnetic interaction, one intramolecular 3d(Cu^{II})–4f(Pr^{III}) magnetic interaction and one intramolecular 4f(Pr^{III})–4f(Pr^{III}) magnetic interaction. To determine the values of those couplings, three dinuclear compounds ($\{[Ni(salen)Pr(hfac)_3][Ni(salen)]\}$ (NiPr), $\{[Ni(salen)Pr(hfac)_3(pyr)](CHCl_3)\}$ (NiPrpyr), $[Cu(salen)Pr(hfac)_3(pyr)]$ and (CuPrpyr) and one tetranuclear $\{[\{Cu(salen)Pr(hfac)_3\}_2(bpy)](CHCl_3)_2\}$ (Cu_2Pr_2bpy) compound, all judiciously chosen, are synthesized, and their crystal structures resolved by X-ray diffraction. The nature of all magnetic exchange interactions is determined by using a "comparative method". All $J_{Cu\text{-}Pr}$, $J_{Pr\text{-}Pr}$ and $J_{Cu\text{-}Cu}$ couplings are found to be antiferromagnetic, and the latter

interaction has quantitatively been estimated ($J_{Cu\text{-}Cu}$ = –1.86 cm^{-1}). To the best of our knowledge, this is the first observation of a Cu^{II}–Pr^{III} magnetic exchange interaction transmitted by phenoxido oxygen atoms.

Moreover, the possible coordination of a ligand in the coordination sphere of the $Pr(hfac)_3$ moiety opens new perspectives. In particular, this work shows that nitrogenated ligands modify the crystal-field effect around the lanthanide and its magnetic coupling to other species. Hence, interactions involving Ln^{III} ions may be enhanced by the use of such ligands and even more if paramagnetic couplers like nitronyl nitroxide or 7,7,8,8-tetracyanoquinodimethanido (TCNQ) radicals are substituted to the diamagnetic ligands. This should permit for the building of strongly coupled 4f–3d systems based on light lanthanide ions.

A systematic study of the crystal-field effect around the Ln^{III} ions with such ligands could lead to a better understanding of the energy distribution of the Stark sublevels. A theoretical calculation of the energy distribution of those levels should also be helpful. This may be a key ingredient in the design of complexes with stronger 3d–4f magnetic exchange interactions than those in complexes with Ln^{III} ions in a fully oxygenated surrounding.

Experimental Section

Materials and Physical Measurements: H_2salen, Ni(salen), Cu(salen) and $Pr(hfac)_3{\cdot}3H_2O$ were synthesized according literature methods.[39–40] All other reagents were purchased from Aldrich and used as received.

X-ray data for all compounds were collected at low temperature [150(5) K] with an Oxford Diffraction Xcalibur3 diffractometer by using Mo-K_α radiation (λ = 0.71073 Å). Reflections were collected with a θ Bragg angle in the range, 4.07–22.46, 3.76–22.72, 3.98–27.25, 3.96–22.72, 4.05–28.36 and 3.89–22.99°, respectively for NiPr, CuPr, NiPrpyr, CuPrpyr, Cu_2Pr_2bpy and Cu_2Pr_2pyz. Data reductions were accomplished by using CRYSALIS.RED p171.29.2. Absorption correction was performed with both the ABSGRAB and ABSPACK software programmes included in the Crysalis package.[41] The ABSGRAB correction allows the determination of the parameter μ (reported in Table 2). The structures were solved by direct methods, developed by successive difference Fourier syntheses and refined by full-matrix least-squares on all F^2 data by using SHELXL 97.[42] Hydrogen atoms were included in calculated positions and allowed to ride on their parent atoms. CCDC-751409, -751410, -751411, -751412, -751413, -751414 contain the supplementary crystallographic data for CuPr, Cu_2Pr_2bpy, CuPrpyr, Cu_2Pr_2pyz, NiPr and NiPrpyr, respectively, for this paper. These data can be obtained free of charge from The Cambridge Crystallographic Data Centre via www.ccdc.cam.ac.uk/data_request/cif.

The dc-magnetic susceptibility measurements were performed on single crystals slightly crunched with a Cryogenic S600 SQUID magnetometer between 2 and 300 K in an applied magnetic field of 0.2 T for temperatures of 2–250 K and 1 T for temperatures of 250–300 K. These measurements were all corrected for the diamagnetic contribution as calculated with Pascal's constants.

Synthesis for the Compounds NiPr, CuPr, NiPrpyr, CuPrpyr, Cu_2Pr_2bpy and Cu_2Pr_2pyz

NiPr: Ni(salen) (15.9 mg, 0.049 mmol) was dissolved in $CHCl_3$ (5 mL) at 60 °C. After the solution was stirred for 10 min, a solution of $CHCl_3$ (5 mL) containing $Pr(hfac)_3{\cdot}3H_2O$ (40.8 mg, 0.05 mmol) was added. The resulting solution was stirred at reflux for 1 h. Slow evaporation of the crude solution gave unstable orange single crystals. Recrystallization of the previous crystals in 1,2-dichlorethane at 80 °C led to the formation of stable dark-orange single crystals of NiPr. Yield: 43.4 mg (62%). $C_{47}H_{33}F_{18}N_4Ni_2O_{11}Pr$ (1429.3): calcd. C 39.46, H 2.31, N 3.92; found C 39.39, H 2.40, N 3.94.

CuPr: Cu(salen) (16.0 mg, 0.049 mmol) was dissolved in $CHCl_3$ (5 mL) at 60 °C, and a solution of $CHCl_3$ (5 mL) containing $Pr(hfac)_3{\cdot}3H_2O$ (40.8 mg, 0.05 mmol) was added. The resulting solution was stirred at reflux for 1 h. Slow evaporation of the crude solution gave red single crystals of CuPr. Yield: 38.0 mg (71%). $C_{31}H_{17}CuF_{18}N_2O_8Pr$ (1091.4): calcd. C 34.08, H 1.56, N 2.57; found C 34.19, H 1.59, N 2.50.

NiPrpyr: Ni(salen) (15.9 mg, 0.049 mmol) was dissolved in $CHCl_3$ (5 mL) at 60 °C. After the solution was stirred for 10 min, a solu-

Table 2. Crystallographic data.

	NiPr	CuPr	NiPrpyr	CuPrpyr	Cu_2Pr_2bpy	Cu_2Pr_2pyz
Formula	$C_{47}H_{33}F_{18}N_4Ni_2O_{11}Pr$	$C_{62}H_{34}Cu_2F_{36}N_4O_{16}Pr_2$	$C_{35}H_{22}Cl_3F_{18}N_4NiO_8Pr$	$C_{34}H_{21}CuF_{18}N_4O_8Pr$	$C_{74}H_{44}Cl_6Cu_2F_{36}N_6O_{16}Pr_2$	$C_{66}H_{44}Cu_2F_{36}N_6O_{19}Pr_2$
F_w [g mol^{-1}]	1429.3	2182.8	1274.1	1159.3	2577.8	2316.8
a [Å]	13.301(1)	16.924(1)	12.899(1)	31.591(4)	11.1759(6)	22.113(5)
b [Å]	30.173(3)	22.602(2)	13.099(1)	18.730(2)	12.2802(6)	16.585(5)
c [Å]	13.415(2)	19.417(2)	14.378(1)	16.803(2)	17.2780(9)	23.396(5)
α [°]	90	90	78.590(8)	90	99.273(4)	90
β [°]	95.941(5)	90.444(7)	73.685(8)	120.568(14)	95.504(4)	91.314(5)
γ [°]	90	90	80.618(7)	90	91.837(4)	90
V [Å^3]	5355(3)	7427(3)	2270.5(3)	8561(5)	2327(2)	8578(4)
Z	4	4	2	8	1	4
Space group	*Cc* (No. 9)	$P2_1/n$ (No. 14)	$P\bar{1}$ (No. 2)	*C*2/*c* (No. 15)	$P\bar{1}$ (No. 2)	*C*2/*c* (No. 15)
T [K]	150(2)	150(2)	150(2)	150(2)	150(2)	150(2)
λ [Å]	0.71073	0.71073	0.71073	0.71073	0.71073	0.71073
$\rho_{calcd.}$ [g cm^{-3}]	1.771	1.975	1.864	1.800	1.840	1.790
μ [cm^{-1}]	17.15	20.12	17.78	17.52	17.88	17.50
R_1	0.0443	0.0591	0.0509	0.0766	0.0544	0.0618
wR_2	0.0688	0.1313	0.1323	0.1935	0.1373	0.1491

tion of $CHCl_3$ (5 mL) containing $Pr(hfac)_3{\cdot}3H_2O$ (40.8 mg, 0.05 mmol) was added. The resulting solution was stirred at reflux for 1 h. A solution of $CHCl_3$ (5 mL) containing pyrazole (6.8 mg, 0.1 mmol) was then added. The resulting mixture was stirred at reflux for one additional hour. The crude solution was slowly evaporated to form orange–red single crystals of NiPrpyr. Yield: 36.8 mg (65%). One of these crystals was rapidly selected and mounted on the diffractometer to collect the data. No decrease in the diffraction data intensities was observed during collection to 150 K. Single crystals were found to become amorphous after 1 h at room temperature by loss of solvent molecules. $C_{34}H_{21}F_{18}N_4NiO_8Pr$ (1154.6): calcd. C 35.34, H 1.82, N 4.85; found C 34.99, H 1.71, N 4.77.

CuPrpyr: The operating method was similar to that used for NiPrpyr, with the exception that Cu(salen) (16 mg) was used instead of Ni(salen). Slow evaporation of the mixture led to the formation of prismatic purple single crystals of CuPrpyr. Yield: 50.0 mg (88%). These crystals were stable in air at room temperature. $C_{34}H_{21}CuF_{18}N_4O_8Pr$ (1159.4): calcd. C 35.19, H 1.81, N 4.83; found C 35.11, H 1.83, N 4.80.

Cu_2Pr_2bpy: The operating method was similar to that used for CuPrpyr, with the exception that 4,4′-bipyridine (7.8 mg, 0.05 mmol) was used instead of pyrazole. Slow evaporation of the mixture led to the formation of dark-pink single crystals of Cu_2Pr_2bpy. Yield: 65.7 mg (52%). These crystals were stable for about one week in air at room temperature and for more than one month at 250 K. $C_{74}H_{44}Cl_6Cu_2F_{36}N_6O_{16}Pr_2$ (2577.8): calcd. C 34.45, H 1.71, N 3.26; found C 34.77, H 1.82, N 3.34.

Cu_2Pr_2pyz: The operating method was similar to that used for Cu_2Pr_2bpy, with the exception that pyrazine (4.0 mg, 0.05 mmol) was used instead of 4,4′-bipyridine. Slow evaporation of the mixture led to the formation of pink single crystals of Cu_2Pr_2pyz. Yield: 64.7 mg (57%). $C_{66}H_{44}Cu_2F_{36}N_6O_{19}Pr_2$ (2316.8): calcd. C 34.19, H 1.90, N 3.63; found C 34.58, H 1.97, N 3.59.

Supporting Information (see footnote on the first page of this article): ORTEP view, crystal packing and selected distances for CuPr are presented.

Acknowledgments

We acknowledge financial support from the Italian Ministry of University and Scientific and Technological Research (MURST) [Foreign Investment Review Board (FIRB) and Partnership for Rural Inverness & Nairn (PRIN) grants], from the European Union through the Human Potential Program RTN-QUELMOLNA (MRTN-CT-2003–504880) and from the NE-MAG-MANET (NMP3-CT-2005-515767). F. P. thanks the German Deutschen Forschungsgemeinschaft (DFG) (SPP1137) for his post-doctoral fellowship. S. Ciattini is acknowledged for his help with the crystallographic measurements.

[1] a) D. Gatteschi, R. Sessoli, J. Villain, *Molecular Nanomagnets*; Oxford University Press, Oxford, U. K., **2006**; T. Lis, *Acta Crystallogr., Sect. Acta Crystallogr., Sect. B* **1980**, *36*, 2042–2046; b) R. Sessoli, H. L. Tsai, A. R. Schake, S. Wang, J. B. Vincent, K. Folting, D. Gatteschi, G. Christou, D. N. Hendrickson, *J. Am. Chem. Soc.* **1993**, *115*, 1804–1816; c) G. Christou, D. Gatteschi, D. N. Hendrickson, R. Sessoli, *MRS Bull.* **2000**, *25*, 66–71; d) S. Accorsi, A.-L. Barra, A. Caneschi, G. Chastanet, A. Cornia, A. C. Fabretti, D. Gatteschi, C. Mortalo, E. Olivieri, F. Parenti, P. Rosa, R. Sessoli, L. Sorace, W. Wernsdorfer, L. Zobbi, *J. Am. Chem. Soc.* **2006**, *127*, 4742–4755.

[2] a) F. Mori, T. Ishida, T. Nogani, *Polyhedron* **2005**, *24*, 2588–2592; b) F. Mori, T. Nyui, T. Ishida, T. Nogami, K.-Y. Choi, H. Nojiri, *J. Am. Chem. Soc.* **2006**, *128*, 1440–1441; c) A. Mishra, W. Wernsdorfer, K. A. Abboud, G. Christou, *J. Am. Chem. Soc.* **2004**, *126*, 15648–15649; d) S. Osa, T. Kido, N. Matsumoto, N. Re, A. Pochaba, J. Mrozinski, *J. Am. Chem. Soc.* **2004**, *126*, 420–421; e) C. M. Zaleski, F. C. Depperman, J. W. Kampf, M. L. Kirk, V. L. Pecoraro, *Angew. Chem. Int. Ed.* **2004**, *43*, 3912–3914; *Angew. Chem.* **2004**, *116*, 4002–4004; f) M. Murugesu, A. Mishra, W. Wernsdorfer, K. A. Abboud, G. Christou, *Polyhedron* **2006**, *25*, 613–625; g) M. Ferbinteanu, T. Kajiwara, K.-Y. Choi, H. Nojiri, A. Nakamoto, N. Kojima, F. Cimpoesu, Y. Fujimura, S. Takaishi, M. Yamashita, *J. Am. Chem. Soc.* **2006**, *128*, 9008–9009; h) C. Aronica, G. Pilet, G. Chastanet, W. Wernsdorfer, J.-F. Jacquot, D. Luneau, *Angew. Chem. Int. Ed.* **2006**, *45*, 4659–4662; *Angew. Chem.* **2006**, *118*, 4775–4778; i) F. Pointillart, K. Bernot, R. Sessoli, D. Gatteschi, *Eur. J. Chem.* **2006**, *13*, 1602–1609.

[3] a) O. Guillou, P. Bergerat, O. Kahn, E. Bakalbassis, K. Boubekeur, P. Batail, M. Guillot, *Inorg. Chem.* **1992**, *31*, 110–114; b) O. Guillou, O. Kahn, R. L. Oushoorn, K. Boubekeur, P. Batail, *Inorg. Chim. Acta* **1992**, *198–200*, 119–131.

[4] a) F. Bartolomé, J. Bartolomé, R. L. Oushoorn, O. Guillou, O. Kahn, *J. Magn. Magn. Mater.* **1995**, *140–144*, 1711; b) M. Evangelisti, F. Bartolomé, J. Bartolomé, M. L. Kahn, O. Kahn, *J. Magn. Magn. Mater.* **1999**, *196*, 584–585.

[5] a) M. Andruh, I. Ramade, E. Codjovi, O. Guillou, O. Kahn, J. C. Trombe, *J. Am. Chem. Soc.* **1993**, *115*, 1822–1829; b) J. L. Sanz, R. Ruiz, A. Gleizes, F. Lloret, J. Faus, M. Julve, J. J. Borras-Almenar, Y. Journaux, *Inorg. Chem.* **1996**, *35*, 7384–7393; c) K. Manseki, M. Kumagai, M. Sakamoto, H. Sakiyama, Y. Nishida, A. Matsumoto, Y. Sadaoka, M. Ohba, H. Okawa, *Bull. Chem. Soc. Jpn.* **1998**, *71*, 379–383.

[6] a) J.-P. Costes, F. Dahan, A. Dupuis, *Inorg. Chem.* **2000**, *39*, 5994–6000; b) J.-P. Costes, J. M. Juan-Clemente, F. Dahan, J. Milon, *Inorg. Chem.* **2004**, *43*, 8200–8202; c) J.-P. Costes, M. Auchel, F. Dahan, V. Peyrou, S. Shova, W. Wernsdorfer, *Inorg. Chem.* **2006**, *45*, 1924–1934.

[7] J.-P. Costes, F. Dahan, W. Wernsdorfer, *Inorg. Chem.* **2006**, *45*, 5–7.

[8] a) J.-P. Costes, F. Dahan, A. Dupuis, J.-P. Laurent, *Inorg. Chem.* **1996**, *35*, 2400–2402; b) J.-P. Costes, F. Dahan, A. Dupuis, J.-P. Laurent, *Inorg. Chem.* **1997**, *36*, 3429–3433; c) J.-P. Costes, F. Dahan, A. Dupuis, J.-P. Laurent, *Inorg. Chem.* **2000**, *39*, 165–168; d) J.-P. Costes, J. M. Juan-Clemente, F. Dahan, F. Dumestre, J.-P. Tuchagues, *Inorg. Chem.* **2002**, *41*, 2886–2891; e) M. L. Kahn, T. M. Rajendiran, Y. Jeannin, C. Mathonière, O. Kahn, *C. R. Acad. Sci. Paris, Série IIc, Chimie/Chemistry* **2000**, *3*, 131.

[9] A. Bencini, C. Benelli, A. Caneschi, R. L. Carlin, A. Dei, D. Gatteschi, *J. Am. Chem. Soc.* **1985**, *107*, 8128–8136.

[10] a) R. E. P. Winpenny, *Chem. Soc. Rev.* **1998**, *27*, 447–452; M. Sakamoto, K. Manseki, H. Ohkawa, *Coord. Chem. Rev.* **2001**, *219–221*, 379–414; b) R. Koner, G.-H. Lee, Y. Wang, H.-H. Wei, S. Mohanta, *Eur. J. Inorg. Chem.* **2005**, *8*, 1500–1505; S. Mohanta, H.-H. Lin, C.-J. Lee, H.-H. Wei, *Inorg. Chem. Commun.* **2002**, *5*, 585–588.

[11] I. Ramade, O. Kahn, Y. Jeannin, F. Robert, *Inorg. Chem.* **1997**, *36*, 930–936.

[12] a) M. Sasaki, K. Manseki, H. Horiuchi, M. Kumagai, M. Sakamoto, H. Nishida, Y. Sakiyama, M. Sakai, Y. Sadaoka, M. Ohba, H. Ohkawa, *J. Chem. Soc., Dalton Trans.* **2000**, 259–263; b) C. Benelli, M. Murrie, S. Parson, *J. Chem. Soc., Dalton Trans.* **1999**, 4125–4126.

[13] a) A. Figuerola, C. Diaz, J. Ribas, V. Tangoulis, J. Granell, F. Lloret, J. Mahia, M. Maestro, *Inorg. Chem.* **2003**, *42*, 641–649; b) J.-P. Costes, F. Dahan, B. Donnadieu, J. Garcia-Tojal, J.-P. Laurent, *Eur. J. Inorg. Chem.* **2001**, 363–365; c) J.-P. Costes, F.

Dahan, A. Dupuis, J.-P. Laurent, *Inorg. Chem.* **2000**, *39*, 169–173.
[14] a) M. L. Kahn, C. Mathonière, O. Kahn, *Inorg. Chem.* **1999**, *38*, 3692–3697; b) J.-P. Costes, F. Dahan, A. Dupuis, J.-P. Laurent, *Chem. Eur. J.* **1998**, *4*, 1616–1620.
[15] M. L. Kahn, J.-P. Sutter, S. Golhen, P. Guionneau, L. Ouahab, O. Kahn, D. Chasseau, *J. Am. Chem. Soc.* **2000**, *122*, 3413–3421.
[16] a) E. A. Boudreaux, L. N. Mulay, *Theory and Applications of Molecular Paramagnetism*, John Wiley, New York, **1976**; b) A. Herpin, *Théorie du Magnétisme*, Press. Univ. France, Paris, **1968**.
[17] O. Kahn, *Molecular Magnetism*, VCH, Weinheim, **1993**.
[18] J.-P. Sutter, M. L. Kahn, "*Magnetism: Molecules to Materials V*", VCH, Weinheim, **2005**.
[19] J.-P. Sutter, M. L. Kahn, O. Kahn, *Adv. Mater.* **1999**, *11*, 863–865.
[20] M. L. Kahn, P. Lecante, M. Verelst, C. Mathonière, O. Kahn, *Chem. Mater.* **2000**, *12*, 3073–3079.
[21] T. Kido, Y. Ikuta, Y. Sunatsuki, Y. Ogawa, N. Matsumoto, *Inorg. Chem.* **2003**, *42*, 398–408.
[22] A. Caneschi, A. Dei, D. Gatteschi, S. Poussereau, L. Sorace, *Dalton Trans.* **2004**, 1048–1055.
[23] R. Koner, H.-H. Lin, H.-H. Wei, S. Mohanta, *Inorg. Chem.* **2005**, *44*, 3524–3536.
[24] M. L. Kahn, R. Ballou, P. Porcher, O. Kahn, J.-P. Sutter, *Chem. Eur. J.* **2002**, *8*, 525–531.
[25] P. Porcher, M. C. Dos Santos, O. Malta, *Phys. Chem. Chem. Phys.* **1999**, *1*, 397–405.
[26] J. C. Bünzli in *Lanthanide Probes in Life, Chemicals and Earth Sciences: Theory and Practice* (Eds.: J. C. G. Bünzli, G. R. Choppin), Elsevier, Amsterdam, **1989**, p. 219.
[27] D. Luneau, G. Risoan, P. Rey, A. Grand, A. Caneschi, D. Gatteschi, J. Laugier, *Inorg. Chem.* **1993**, *32*, 5616–5622.
[28] W. Partenheimer, R. S. Drago, *Inorg. Chem.* **1970**, *9*, 47–52.
[29] M. Sasaki, K. Manseki, H. Horiuchi, M. Kumagai, M. Sakamoto, H. Sakiyama, Y. Nishida, M. Sakai, Y. Sadaoka, M. Ohba, H. Okawa, *J. Chem. Soc., Dalton Trans.* **2000**, 259–263.
[30] D. R. Van Staveren, G. A. Van Albada, J. G. Haasnoot, H. Kooijaman, A. M. Manotti Lanfredi, P. J. Nieuwenhuizen, A. L. Spek, F. Ugozzoli, T. Weyhermüller, J. Reedijk, *Inorg. Chim. Acta* **2001**, *315*, 163–171.
[31] C. K. Johnson, *ORTEP, Report ORNL-5138*, Oak Ridge National Laboratory, Oak Ridge, TN, **1976**.
[32] R. B. King, *J. Am. Chem. Soc.* **1969**, *91*, 7211–7216.
[33] R. Gheorghe, P. Cucos, M. Andruh, J.-P. Costes, B. Donnadieu, S. Shova, *Chem. Eur. J.* **2006**, *12*, 187–203.
[34] E. Furet, K. Costuas, P. Rabiller, O. Maury, *J. Am. Chem. Soc.* **2008**, *130*, 2180–2183.
[35] M. M. Bhadbhade, D. Srinivas, *Inorg. Chem.* **1993**, *32*, 5458–5466.
[36] J. D. Rinehart, T. D. Harris, S. A. Kozimor, B. M. Bartlett, J. R. Long, *Inorg. Chem.* **2009**, *48*, 3382–3395.
[37] H. Miyasaka, R. Clérac, T. Ishii, H.-C. Chang, S. Kitagawa, M. Yamashita, *J. Chem. Soc., Dalton Trans.* **2002**, 1528–1534.
[38] E. Pardo, J. Faus, M. Julve, F. Lloret, M. C. Munoz, J. Cano, X. Ottenwaelder, Y. Journaux, R. Carrasco, G. Blay, I. Fernandez, R. Ruiz-Garcia, *J. Am. Chem. Soc.* **2003**, *125*, 10770–10771.
[39] R. H. Bailes, M. Calvin, *J. Am. Chem. Soc.* **1947**, *69*, 1886–1893.
[40] M. F. Richardson, W. F. Wagner, D. E. J. Sands, *J. Inorg. Nucl. Chem.* **1968**, *30*, 1275–1290.
[41] *CrysAlis CDD* and *CrysAlis RED version p 171.29.2*, Oxford diffraction, Oxfordshire, Great Britain, **2000**.
[42] G. M. Sheldrick, *SHELXL-97, Program for Refinement of Crystal Structures*, University of Göttingen, Germany, **1997**.

Received: October 16, 2009
Published Online: January 15, 2010

